NeuroImage 146 (2017) 869–882

Contents lists available at ScienceDirect

NeuroImage

journal homepage: www.elsevier.com/locate/neuroimage

Neurovascular unit remodelling in the subacute stage of stroke recovery

Evelyn M.R. Lake[a,*], Paolo Bazzigaluppi[b,c], James Mester[a], Lynsie A.M. Thomason[b], Rafal Janik[a], Mary Brown[d], JoAnne McLaurin[d], Peter L. Carlen[c,e], Dale Corbett[f,g], Greg J. Stanisz[a,b,h], Bojana Stefanovic[a,b,g,i]

[a] Department of Medical Biophysics, University of Toronto, ON, Canada
[b] Physical Sciences, Sunnybrook Research Institute, Toronto, ON, Canada
[c] Neurobiology, Toronto Western Research Institute, Toronto, ON, Canada
[d] Department of Laboratory Medicine and Pathobiology, University of Toronto, Ontario, Canada
[e] Department of Medicine and Physiology, University of Toronto, Toronto, ON, Canada
[f] Faculty of Cellular and Molecular Medicine, University of Ottawa, ON, Canada
[g] Heart and Stroke Foundation Centre for Stroke Recovery, Canada
[h] Department of Neurosurgery and Paediatric Neurosurgery, Medical University Lublin, Lublin, Poland
[i] Neuropsychopharmacology Research Group, Sunnybrook Research Institute, Toronto, ON, Canada

ARTICLE INFO

Keywords:
Focal ischaemia
Endothelin-1
Preclinical stroke modelling
Magnetic resonance imaging
Arterial spin labelling
Montoya reaching task
Intra-cranial electrophysiology
Immunofluorescence

ABSTRACT

Brain plasticity following focal cerebral ischaemia has been observed in both stroke survivors and in preclinical models of stroke. Endogenous neurovascular adaptation is at present incompletely understood yet its potentiation may improve long-term functional outcome. We employed longitudinal MRI, intracranial array electrophysiology, Montoya Staircase testing, and immunofluorescence to examine function of brain vessels, neurons, and glia in addition to forelimb skilled reaching during the subacute stage of ischemic injury progression. Focal ischemic stroke (~100 mm^3 or ~20% of the total brain volume) was induced in adult Sprague-Dawley rats via direct injection of endothelin-1 (ET-1) into the right sensori-motor cortex, producing sustained impairment in left forelimb reaching ability. Resting perfusion and vascular reactivity to hypercapnia in the peri-lesional cortex were elevated by approximately 60% and 80% respectively seven days following stroke. At the same time, the normal topological pattern of local field potential (LFP) responses to peripheral somatosensory stimulation was abolished and the average power of spontaneous LFP activity attenuated by approximately 50% relative to the contra-lesional cortex, suggesting initial response attenuation within the peri-infarct zone. By 21 days after stroke, perilesional blood flow resolved, but peri-lesional vascular reactivity remained elevated. Concomitantly, the LFP response amplitudes increased with distance from the site of ET-1 injection, suggesting functional remodelling from the core of the lesion to its periphery. This notion was further buttressed by the lateralization of spontaneous neuronal activity: by day 21, the average ipsi-lesional power of spontaneous LFP activity was almost twice that of the contra-lesional cortex. Over the observation period, the peri-lesional cortex exhibited increased vascular density, along with neuronal loss, astrocytic activation, and recruitment and activation of microglia and macrophages, with neuronal loss and inflammation extending beyond the peri-lesional cortex. These findings highlight the complex relationship between neurophysiological state and behaviour and provide evidence of highly dynamic functional changes in the peri-infarct zone weeks following the ischemic insult, suggesting an extended temporal window for therapeutic interventions.

1. Introduction

Although ischemic stroke is the leading cause of adult disability worldwide, most stroke survivors report some improvement with time and some show significant recovery even in the absence of treatment (Seil 1997; Steinberg and Augustine, 1997; Hallett, 2001; Krishnamurthi et al., 2013). Recent work has investigated the determinants of prognosis post stroke and there is widespread recognition of the importance of understanding the mechanisms of endogenous recovery as a means of guiding the development of new treatments (Lee and van Donkelaar, 1995; Seil, 1997; Steinberg and Augustine, 1997; Hallett 2001). A prominent topic of current enquiry is injury-induced vascular remodelling. An increase in vascular density on post-mortem neuropathological examination in stroke patients correlates

* Correspondence to: Department of Radiology and Biomedical Imaging, The Anlyan Center, 300 Cedar Street New Haven CT, 06520-8043, Canada.
E-mail addresses: evelyn.lake@mail.utoronto.ca, evelyn.lake@yale.edu (E.M.R. Lake).

http://dx.doi.org/10.1016/j.neuroimage.2016.09.016
Received 10 June 2016; Accepted 8 September 2016
Available online 21 September 2016
1053-8119/

with functional improvement and longer survival after ischemic injury (Krupiński et al., 1992, 1994; Szpak et al. 1999). A number of preclinical studies have reported that histopathological evidence of angiogenesis correlates with transient in vivo increases in cerebral blood flow (CBF) and/or cerebral blood volume (CBV) in the peri-lesional tissue during the subacute phase (one to three weeks following stroke) (Lin et al., 2002; Dijkhuizen et al., 2003; Lin et al., 2008; Hayward et al., 2011; Martin et al., 2012; Chang et al., 2013). In preclinical models, a transition from hypo- (in the initial 24–48 h) to hyper-perfusion is associated with angiogenesis one to two weeks following injury (Dijkhuizen et al., 2003; Hayward et al., 2011; Zhang et al., 2013) and improved performance on neurological test batteries, beam walking and cylinder tests (Lin et al., 2002; Dijkhuizen et al., 2003; Lin et al., 2008; Hayward et al., 2011; Martin et al., 2012; Zhang et al., 2013). The details of spatio-temporal changes in neurovascular morphology and function post ischaemia remain uncertain yet are critical for the design of more effective therapeutic approaches in the subacute stage of stroke.

To address this gap, we injected endothelin-1 (ET-1), a potent vasoconstrictor, into the forelimb region of the right sensorimotor cortex to produce a robust, focal region of ischaemia. The ET-1 model was chosen as it produces a spatially targeted, focal lesion, similar in volume to what is observed in stroke survivors (Carmichael, 2005); and exhibits flow impairment and resolution kinetics similar to those observed in human stroke (Olsen and Lassen, 1984; Mohr et al., 1986; Heiss et al., 2000; Biernaskie et al., 2001; Carmichael, 2005). Brain morphology and vascular function were assessed using *in situ* T_2-weighted magnetic resonance imaging (MRI) and continuous arterial spin labelling (CASL) functional MRI; neuronal activity was evaluated using intracortical array electrophysiology, and neuronal, glial, and vascular morphology were assessed using pathological analysis. These biological assays were related to skilled reaching ability on the Montoya Staircase test. Assays were conducted over 21 days following ischemic insult to examine the evolution of functional and structural changes in the neurovascular unit.

2. Methods

All animals within this study were adult male Sprague-Dawley rats. All data processing was performed blinded to surgery group allocation (stroke or sham) and injury status (seven or 21 days after stroke or sham-surgery). Inclusion criteria are summarized in Supplementary Table 1 for each assay.

2.1. Stroke induction

All animals underwent the same stroke induction or sham surgical procedure under isoflurane anaesthesia (5% induction and 2–2.5% maintenance). Animals were secured in a small animal stereotaxic apparatus (David KOPF Instruments, Tujunga California, USA). Under aseptic condition, a midline incision was made, and two burr holes, 0.8 mm in diameter, drilled at 0.0 mm A-P (anterior-posterior), −2.5 mm M-L (medial-lateral); and at 2.3 mm A-P, −2.5 mm M-L over the right sensorimotor cortex using a high-speed micro-drill (Foredom Electric Co., Bethel Connecticut, USA). A 10 μl Hamilton Syringe (Model 80366, needle size 26 s gauge with beveled tip) was used to inject 800 picomoles of ET-1 (Sigma-Aldrich, St. Louis Missouri, USA) suspended in 4 μl of phosphate buffered saline (PBS) or PBS alone (sham-surgery) at −2.3 mm D-V (dorsal-ventral). One 2 μl aliquot was injected at each location, for a total of 4 μl. After lowering the needle to −2.5 mm and retracting to −2.3 mm D-V, a one-minute delay was allowed before injection began. A further one-minute delay was kept between the delivery of each μl, and a two-minute delay preceded needle retraction. Injections were made at a rate of 1 μl/min, for a total delivery time (including 4 one-minute delays, and 2 two-minute delays) of 12 min. Burr holes were closed with bone wax and the scalp sutured over the skull. For analgesia, animals were given a subcutaneous dose of Marcaine (0.2 mg/kg) at the beginning and end of surgery (Windle et al., 2006).

2.2. Magnetic resonance imaging

All animals were imaged seven and 21 days following stroke induction or sham-surgery on a 7T animal system (Bruker, BioSpec, Etlingen, Germany). Animals were immobilized with ear bars and an incisor bar, and a stable plane of anaesthesia maintained with an intravenous infusion of 45 mg/kg/hr of propofol (Pharmascience Inc., Montreal Quebec, Canada). Propofol anaesthesia was chosen in light of its being well tolerated and allowing rapid recovery, thus being well suited to longitudinal experiments; in addition to having been successfully used for cerebral blood flow quantification via ASL in rats (Griffin et al., 2010).

2.2.1. T_2-weighted MRI

A birdcage body coil was used for signal excitation and a quadrature receive-only coil for signal detection. Forty-five coronal images were obtained with a rapid acquisition with relaxation enhancement (RARE) sequence (RARE factor of eight, repetition time/echo time TR/TE of 5500/47 ms, and a matrix size of 128×256), with a nominal in-plane spatial resolution of 0.1×0.1 mm^2 and a slice thickness of 0.5 mm in under 12 min. Images were imported into ImageMagick [ImageMagick Studio LLC, 2013. http://www.imagemagick.org/script/index.php] for semi-automated segmentation. Following earlier work (Neumann-Haefelin et al., 2000; Virley et al., 2000; Kidwell et al., 2003; van der Zijden et al., 2008; Jiang et al., 2006), stroke regions were segmented using a predetermined signal intensity threshold of greater than two standard deviations (SDs) above the mean contra-lesional cortical signal intensity. Following segmentation, stroke volumes were calculated for each time point for each animal.

2.2.2. CASL

A custom built labelling coil was positioned at the level of the carotid arteries and a quadrature receive-only coil was used for signal detection. Using a 1.5-s adiabatic labelling pulse, and a 0.4-s post-labelling delay, single-average, single-shot echo-planar images (EPI) were obtained from five 1.5 mm thick coronal slices positioned over the sensorimotor cortex, with a 0.25×0.25 mm^2 in-plane resolution, TR/TE of 2000/8.3 ms, and inter-slice gap of 0.5 mm. Sixty EPI frames were collected to estimate resting perfusion. For vessel reactivity measurements, animals were tracheostomized, mechanically ventilated, and challenged by six presentations of a hypercapnic mixture in ON:OFF periods of 1:4 min (ON: 10% CO_2, 31% O_2 and 59% N_2, OFF: 0% CO_2, 31% O_2 and 69% N_2). Inspired mixture composition and delivery were controlled by a programmable GasMixer (GSM-3, CWE Inc., Boston MA).

2.2.3. CASL data processing

All CASL data were motion corrected (AFNI, Analysis of Functional NeuroImages (Cox, 1996), *2dImReg*), masked (to isolate grey matter), and spatially blurred within the grey matter mask (AFNI *3dBlurToFWHM*, full-width-half-maximum 0.55 mm) prior to fitting the data using a Generalized Linear Model (AFNI *3dDeconvolve*). Subject-specific hemodynamic response functions were produced by averaging the signal in the left (contra-lateral) cortical grey matter (Kang et al., 2003). A threshold was applied to resulting maps of perfusion signal changes elicited by hypercapnia and resting perfusion to correct for multiple comparisons (false discovery rate $q < 0.01$). In each animal, we manually identified a training set of approximately 40–60 voxels in both perfusion response and resting perfusion maps residing in the contra- and ipsi-lateral cortices. The pial surface and boundary with corpus callosum were excluded, along with major vessels. Using these training data, classification was performed with a

probabilistic classifier (MINCTools, (Neelin and Fonov et al.), *Classify*) and thresholds applied to the resulting probabilistic maps: at >80% a posteriori probability of belonging to the left cortex (contralateral region of interest, ROI) and at >75% a posteriori probability of belonging to the affected right cortex (ipsilateral ROI). The CASL measurements were then reported in terms of the right-to-left ratio following earlier work (Heiss et al., 1997; Shen et al., 2011; Hayward et al., 2011; Wegener et al., 2006), given the presence of nuisance signal variability sources that affect both hemispheres equally, including inter-subject variability in T_1, inversion efficiency, and global responses to anaesthesia. Notwithstanding, to explore the effect of ischaemia on the left (contralateral) sensorimotor cortex hemodynamics, the contralateral CASL data variation in relation to the average non-lesioned whole brain grey matter signal were also examined.

2.3. Behavioural testing

Each animal was placed in a staircase test box designed so that food pellets from the left staircase steps could only be retrieved with the left paw and those from the right set of steps with the right paw. During each trial, three Noyes precision pellets (45 mg, Research Diets Inc, New Brunswick NJ) were placed on each of the 14 steps, seven on each side of the box. Animals were allowed 15 min to eat pellets. Whenever a pellet was dropped, it fell to the base of the box where it could not be retrieved. At the conclusion of each trial, the number of uneaten pellets on each side was recorded. To become proficient at the skilled reaching task, animals were trained for two trials per day (with a minimum of three hours between trials) for a period of 10 days prior to stroke induction or sham-surgery. Baseline reaching ability was estimated as the average number of pellets eaten during the final eight consecutive trials (i.e., trials performed on the final four days of the 10-day training period) (Montoya et al., 1991; Windle et al., 2006). Following earlier work, to reach baseline training criteria, animals had to consume, on average across the final eight training trials, at least 12 pellets with each forepaw (Windle et al., 2006). Three days following stroke or sham-surgery, reaching ability was tested twice daily for three consecutive days (on days five, six and seven after surgery). Testing was repeated on days 19, 20 and 21.

2.4. Electrophysiological recordings

Recordings were performed either seven or 21 days following stroke or sham-surgery. Animals were anaesthetised with isofluorane (5% induction and 2–2.5% maintenance) and positioned in a stereotaxic frame (David KOPF Instruments, Tujunga California, USA). Using a high-speed micro-drill (Foredom Electric Co., Bethel Connecticut, USA), skull was removed to expose dura, which was carefully resected, to create two cranial windows over the left and right somatosensory areas (~9.0×4.4 mm in size, extending from 2.0 mm to −7.0 mm in the A-P direction, and from −0.1 mm to −4.5 mm in the M-L direction). Two multi-electrode arrays (MEA – MicroProbes, Gaithersburg Maryland, USA) composed of 16 (28) Pl/Ir electrodes (tip diameter: 125 μm, impedance: 0.5 MΩ, inter-electrode spacing: 250 μm, for a total MEA width of 0.5 mm and a total length of 2 mm) were lowered into the exposed cortices (to 250 μm D-V) for intracortical recordings. The MEA centre was placed at −1.0 mm A-P and −2.5 mm M-L, so as to align the most anterior pair of electrodes with the posterior injection site. After surgery and electrode placement, isoflurane was discontinued and a continuous infusion of α-chloralose (27 mg/kg/hr) begun. Acquisition bandwidth was set to 0.3–5 kHz. Signal was amplified 20× at the head-stage and 50× by the amplifier (Model 3600 – AM-systems, Carlsborg Washington, USA). Data were acquired using a 32-channel SciWorks DataWave Acquisition System (AM-systems, Carlsborg Washington, USA), with a sampling rate of 20 kHz. Local field potential (LFP) responses were extracted off-line by filtering the raw traces with a low-pass filter with a cutoff frequency of 300 Hz. Only events identified as a negative deviation of the field potential larger than three SDs from mean baseline signal amplitude were used in the analysis (cf. Supplementary Fig. 1). Further, we report the fraction of bilateral forepaw stimulations delivered which resulted in above threshold and uncorrupted (by spontaneous activity) LFP responses recorded by the most anterior electrode (at 0.0 mm Bregma, closest to the forelimb representation) cf. Supplementary Fig. 2 and Supplementary Table 2.

2.4.1. Spontaneous activity

One minute of spontaneous activity was recorded before beginning bilateral forepaw stimulation. The Fast Fourier Transform was computed for each two-second interval using a non-over-lapping running window within each channel. Power was normalized between hemispheres by taking the ratio between corresponding channels in each hemisphere (e.g., ipsi-lateral channel #1 divided by contra-lateral channel #1). Following earlier work (Womelsdorf et al., 2014), the channel-wise ipsi- to contra-lateral power ratios were analyzed for each frequency band of interest: Theta (3–10 Hz), Alpha (8–14 Hz), Beta-1 (15–20 Hz), Beta-2 (20–35 Hz) and Gamma (35–90 Hz). These bands have been hypothesized to arise from dynamic motifs that are based on structural circuits and dictate behavioural function, after input-output transformation (Womelsdorf et al., 2014).

2.4.2. Evoked activity

LFP recordings were acquired during bilateral forepaw stimulation (three pulses at 10 Hz, 0.5–0.8 mA) delivered every 10 s and repeated 30 times. The first 10 responses following the presentation of a stimulus and not preceded (within 100 ms) by a spontaneous event were averaged and analyzed. The difference was taken between the average responses of neighbouring channels in a rostro-caudal direction to eliminate signal common to neighbours and isolate signal from the immediate vicinity of each channel. Finally, signal amplitude was normalized for each MEA: the amplitude of the average LFP response in each channel of an MEA was divided by the maximum response amplitude recorded by that MEA. The normalized signal was plotted as a function of distance from Bregma.

2.5. Immunohistochemistry

Following the final MRI session, brains were extracted for immunohistochemical analysis. Animals were euthanized with an over-dose of isoflurane; the brains were removed from the skull, placed in paraformaldehyde (PFA, Sigma-Aldrich, St. Louis, MI) and stored at 4°C. After 24 hrs in PFA, brains were rinsed in PBS and transferred to a 15% sucrose solution and subsequently to a 30% sucrose solution (Sigma-Aldrich, St. Louis, MI). For each primary antibody, six or seven evenly spaced free floating 40 μm coronal sections were collected within the boundaries of the ischemic injury (defined by hyperintensity on *in vivo* T_2-weighted images) between 3.8 mm and -3.5 mm from Bregma in the A-P direction.

Sections were singly labelled with primary antibodies, followed with secondary antibodies conjugated with Alexa 488 fluorescent dye (1/200, Goat Anti-Rabbit A-11008, Donkey Anti-Mouse A-21202, ThermoFisher Scientific, Calgary, AB). The primary antibodies used were GFAP (1/500, Z0334, Dako, Burlington, ON), Iba-1 (1/500, 019-19741, Wako Chemicals, Cape Charles, VA), NeuN (1/200, MAB377, EMD Millipore, Billerica, MA), and RECA-1 (1/100, MCA970R, AbD Serotec Bio-Rad Co, Raleigh, NC). Briefly, frozen cryo-protected sections were transferred to 24 well dishes and washed 3×10 min with PBS. Sections were blocked for one hour at room temperature in PBS containing 2–10% Donkey or Goat Serum and 0.1–0.5% Triton X-100. Sections selected for incubation with Iba-1 antibody were exposed to boiling in 10mM citrate buffer containing 0.05% Tween20 for antigen retrieval prior to blocking. All primary antibodies were diluted in the same blocking buffer and incubated overnight at 4 °C, with the

exception of RECA-1 sections, which were incubated at room temperature.

On the following morning, sections were washed 3×10 min with PBS and then incubated for two hours at room temperature with fluorescent conjugated secondary antibodies diluted in the same blocking buffer. Nuclear counter-stain NucBlue Reagent (DAPI two drops/ml, R37606, Molecular Probes, ThermoFisher Scientific, Calgary, AB) was added at the same time as the secondary antibody. Sections were washed thoroughly in PBS, and mounted on VWR Brand frosted slides with mounting medium (Polyvinyl alcohol mounting medium with DABCO #10981 Sigma-Aldrich, St. Louis, MI) and glass cover-slips.

All sections were digitized on a Zeiss ApoTome.2 Microscope using StereoInvestigator (MBF, Biosciences, Williston, VT) and an air 40× objective (with numerical aperture of 0.95, and working distance of 0.25 mm; Zeiss, Oberkochen, Germany). Each section was registered to the Paxinos and Watson (2005) digital rat brain atlas and ROIs identified based on anatomical locations where increases in GFAP/Iba-1 signal were visually apparent. The ROIs thus identified were: cerebral cortex, caudate putamen, piriform cortex, and olfactory tubercle. The average signal intensity per unit area for each ROI was computed for both hemispheres in all sections stained with GFAP or Iba-1. The ipsi- to contra-lateral inter-hemispheric signal ratio for each ROI was then computed and compared between groups.

For NeuN and RECA-1 stained sections, binary images were generated in ImageJ. A Sobel edge detection filter was first applied to calculate local derivatives along each imaging axis. The edge-enhanced image was then computed by quadrature summation of the two derivatives (Hast, 2014). Next, images were blurred with a Gaussian filter (kernel size of 3 pixels), and the background subtracted (using a sliding paraboloid of 50 pixels) (Sternberg, 1983). Finally, images were binarized using the *Make Binary* algorithm in ImageJ, at a set threshold so that the fractional area occupied by positively stained cells could be computed. The percent of each ROI area occupied by positively stained NeuN or RECA-1 cells was computed and the ipsi- to contra-lateral inter-hemispheric ratio of these values compared between groups.

2.6. Statistical analysis

Linear mixed effect (*lme*) modelling (lme function in R, http://www.R-project.org) was used in the statistical analysis as it is particularly well suited for the present data since it recognizes the relationship between serial observations on the same subjects while allowing for unbalanced groups (here present due to attrition). Lme thus produces robust and sensible restricted maximum likelihood estimates in the presence of unbalanced allocation of subjects by factor (Laird and Ware, 1982). T_2-weighted based lesion volume, CASL data (resting perfusion, and reactivity to 10% CO_2), intracortical electrophysiological recordings (evoked response amplitude and spontaneous activity power), histopathological assays (GFAP, Iba-1, NeuN, and RECA-1), and skilled reaching performance were modelled as linear functions of group (stroke or sham) and time. Subjects were treated as random effects, thus accounting for across-subject variation.

3. Results

All experimental procedures in this study were approved by the Animal Care Committee of the Sunnybrook Research Institute, which adheres to the Policies and Guidelines of the Canadian Council on Animal Care and meets all the requirements of the Provincial Statute of Ontario, Animals for Research Act as well as those of the Canadian Federal Health of Animals Act. Ninety-six (N=65 with stroke and N=31 sham-operated; average weight ± the standard error of the mean (SEM): 383 ± 8 g) adult male Sprague-Dawley rats (Charles River, Montreal, Canada) were included in this study. Animals were housed in pairs on a reversed 12-hr light/dark cycle. MRI, behavioural trials, and electrophysiological recordings were performed during the dark phase. Food and water were freely available except during behavioural trial periods when food was limited to 12–15 g per day (amounting to mild food deprivation). For the duration of the experiments, body weight of each animal was maintained above 90% of free feeding weight.

Continuous monitoring of breath rate, heart rate, blood O_2 saturation, transcutaneous CO_2, end-tidal CO_2 and body temperature was conducted throughout all imaging and electrophysiology experiments (cf. Supplementary Table 3).

3.1. Effect of focal ischaemia on forelimb skilled reaching ability

To evaluate fine motor function before ischaemia and during ischemic injury progression, animals were trained and tested on the Montoya Staircase skilled reaching task, which provides a sensitive measure of forelimb motor performance (Montoya et al., 1991). During the 15-minute task, animals retrieved and ate pellets with either the left or right forelimb. At the conclusion of the task, the number of pellets successfully eaten with each limb was recorded. Fig. 1 shows the number of pellets eaten with the left (contra-lateral) forelimb plotted against time in both stroke and sham groups. All values are quoted as the mean ± SEM.

On average, across eight baseline trials (prior to stroke induction or sham-surgery), animals retrieved 14.9 ± 0.2 pellets (or 71 ± 1% of pellets available) on the left side (N=18). Prior to surgery, there was no difference in performance between cohorts (stroke animals: 14.6 ± 0.3 pellets, 70 ± 1%; sham-operated animals: 15.4 ± 0.3 pellets, 73 ± 1%). One week following surgery, the left forelimb reaching performance of animals with stroke deteriorated to 2.8 ± 0.3 pellets or 13 ± 1% ($P < 0.0001$), while animals that underwent sham surgeries showed no impairment (consuming 14.9 ± 0.3 pellets, or 71 ± 1%). Two weeks later (21 days after stroke or sham-surgery), animals with stroke remained impaired (3.2 ± 0.4 pellets or 15 ± 2%, $P < 0.0001$) while sham-operated animals still performed at baseline level (15.5 ± 0.4, 74 ± 2%). These data demonstrate a substantial decrease in the skilled reaching ability of the contralateral limb in animals with ischemic lesions seven days after injury with no evidence of spontaneous recovery two weeks thereafter; while sham-operated animals showed no effect of surgery or time on reaching performance. Of note, given the extensive preclinical and clinical literature on ipsilateral limb impairment (Wetter et al., 2005; Yarosh et al., 2004; Kwon et al., 2007), the ipsilateral (i.e. right) forelimb also showed a decrease in reaching success following stroke (data not shown), although the ipsilateral deficit was smaller than the contralateral deficit at both seven and 21 days ($P < 0.00001$).

3.2. Spontaneous neuronal activity in the ipsi-lesional cortex

At either seven or 21 days after stroke-induction (or sham-surgery), both somatosensory evoked and spontaneous LFP responses were recorded simultaneously from the right (ipsilateral) and left (contralateral) hemispheres, using a pair of MEAs [in a 2×8 configuration]. Each MEA was placed with the most anterior pair of electrodes in line with the posterior ET-1 or PBS injection site (0.0 Bregma) and the long axis of the array (eight electrodes in length) extending in the A-P direction to +3.0 mm Bregma (Fig. 2a shows the surgical preparation for intracortical electrophysiological recordings of both evoked and spontaneous activity). For a direct measure of neuronal activity, spontaneous LFP events were recorded for one minute prior to recording evoked activity. Following earlier work (Womelsdorf et al., 2014), lateralization (a discrepancy between hemispheres) of spontaneous neuronal activity is reported as the (ipsi- to contra-lateral) ratio of the spectral power in five frequency bands: Theta (3–10 Hz), Alpha

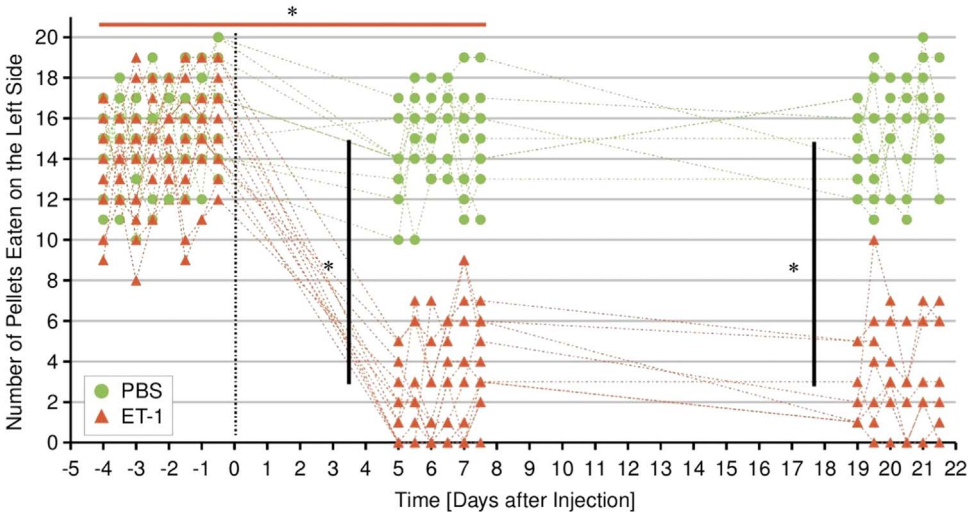

Fig. 1. Montoya Staircase performance. Fig. 1. Pellets eaten during each trial with the contralateral (left) forepaw are shown for each subject for each trial on days five-seven (N=9 stroke, N=9 sham-operated), and 19–21 (N=7 stroke, N=9 sham-operated) after injection. Baseline reaching ability, 14.9 ± 0.2 pellets or 71 ± 1% of pellets available on the left side, was determined based on eight trials prior to surgery (days -5 until -1). At baseline, there was no difference in performance of stroke (14.6 ± 0.3 pellets, 70 ± 1%) and sham animals (15.4 ± 0.3 pellets, 73 ± 1%). There was no time-dependent change in the reaching ability of sham-operated animals: they consumed an average 14.9 ± 0.3 (71 ± 1%) pellets on day seven and 15.5 ± 0.4 (74 ± 2%) pellets on day 21. Stroke caused a decrease in the reaching performance: injured rats consumed 2.8 ± 0.3 (13 ± 1%) ($P < 0.0001$) pellets on day seven and 3.2 ± 0.4 (15 ± 2%) ($P < 0.0001$) pellets on day 21, with no difference in performance between seven and 21 days post stroke. On day seven and 21, ischemic animals consumed fewer pellets with the contralateral forepaw than sham animals ($P < 0.0001$).

(8–14 Hz), Beta-1 (15–20 Hz), Beta-2 (20–35 Hz) and Gamma (35–90 Hz). Fig. 2 depicts MEA positioning (a.); power recorded by each array (ipsi- and contra-lateral) for a representative animal from each group (sham and stroke) (b.i.); the average across each MEA for these animals (b.ii.); and the group-wise ipsi- to contra-lateral ratio average for both time points (c). Table 1 lists the ipsi- to contra-lateral ratios for the five aforementioned frequency bands for both groups.

There was no lateralization of the spectral power in spontaneous activity recordings in sham-operated animals: their average ipsi- to contra-lateral power ratios (across all frequency bands) were 0.98 ± 0.04 (N=5) on day seven and 1.09 ± 0.04 (N=5) on day 21 (refer to Table 1 for results from separate bands). In contrast, stroke animals showed decreased Beta-2 band (20–35 Hz) power, by 51 ± 5%, relative to that of sham animals, on day seven (P=0.03). By 21 days after stroke, the ipsi- to contra-lesional power ratio in stroke animals increased, by an average of 67 ± 9%, indicating a dramatic rise in the ipsi-lesional spontaneous activity. Moreover, the power of ipsi-lesional (relative to contra-lesional) cortical activity on day 21 was higher, by 20 ± 10% than that observed in the sham group. In summary, these data show that an initial silencing in the ipsi-lesional hemisphere progresses to hyperactivity by 21 days after injury.

3.3. Somatotopy in the ipsi-lesional cortex

As the ischemic injury targeted the forelimb representation, forepaw stimulation was employed to assess the effects of ischaemia. The physiological pattern of average normalized response amplitudes as a function of distance (0.0→3.0 mm Bregma) recorded from contralateral (injection naïve) hemispheres seven and 21 days after surgery are shown in Supplementary Fig. 3. Response amplitude (estimated by the magnitude of the first negative peak – N1) was normalized within each MEA by dividing the average amplitude (averaged across the first 10 responses) recorded by each electrode by the amplitude of the largest mean response in that array. The evoked LFP response amplitudes from the contralateral hemispheres followed the expected somatotopic organization, thus getting progressively smaller from 0.0 to +3.0 mm from Bregma in the A-P direction at both time points in the stroke (day seven: N=5 and day 21: N=8) and sham rats (day seven: N=7 and day 21: N=8) ($P < 0.0001$). This decrease in LFP amplitude with distance in the contralateral hemisphere did not depend on either time or group.

Evoked LFP responses in the ipsilateral (injected) hemispheres are shown in Fig. 3. In sham-operated animals, the LFP responses were not distinguishable between hemispheres. In contrast, lesioned hemispheres of stroke animals exhibited evoked LFP response patterns that were distinct from the LFP responses in either the contra-lesional hemispheres of ischemic animals or those in either hemisphere of sham animals ($P < 0.0001$). Seven days post-stroke, the somatotopic organization in ipsi-lesional hemispheres of stroke rats was completely abolished, with no dependence of evoked LFP response amplitude on distance from Bregma. On day 21 post-stroke, intracranial recordings provided evidence of somatotopic remodelling: LFP response amplitude to forelimb stimulation increased with distance from the injection site ($P < 0.0001$). In summary, the results showed that the somatotopic representation in the forelimb cortex was disrupted seven days after ischaemia yet remodelled two weeks later.

The fraction of bilateral stimulations which resulted in above threshold responses recorded by the most anterior electrode (at 0.0mm Bregma, closest to the forelimb representation) were not different between groups at either time point, or between hemispheres in either group, and did not change with time. Across all recordings, an uncorrupted (by spontaneous activity) and above threshold LFP response occurred after 82 ± 13% (mean ± SD) of stimulations in contra-lateral hemisphere, and after 75 ± 13% of stimulations in ipsi-lateral hemisphere (cf. Supplementary Table 2). The inter-hemisphere ratio of the fraction of stimulations which resulted in LFPs used for further analysis averaged across all animals was 0.9 ± 0.1 at 7 and 21 days post surgery (cf. Supplementary Fig. 2).

3.4. Stroke volumes in the ipsi-lesional cortex

To assess the morphological consequences of stroke induction, *in vivo* T_2-weighted MR-images were acquired in all animals seven days after surgery. Supplementary Table 4 lists the stroke volumes in both cohorts, as estimated by hyperintensity on T_2-weighted MRI. Representative *in vivo* T_2-weighted MR-images are shown for one animal from the ischemic group acquired at seven and 21 days after stroke in Supplementary Fig. 4. The volume of stroke remained stable between seven and 21 days across all stroke animals.

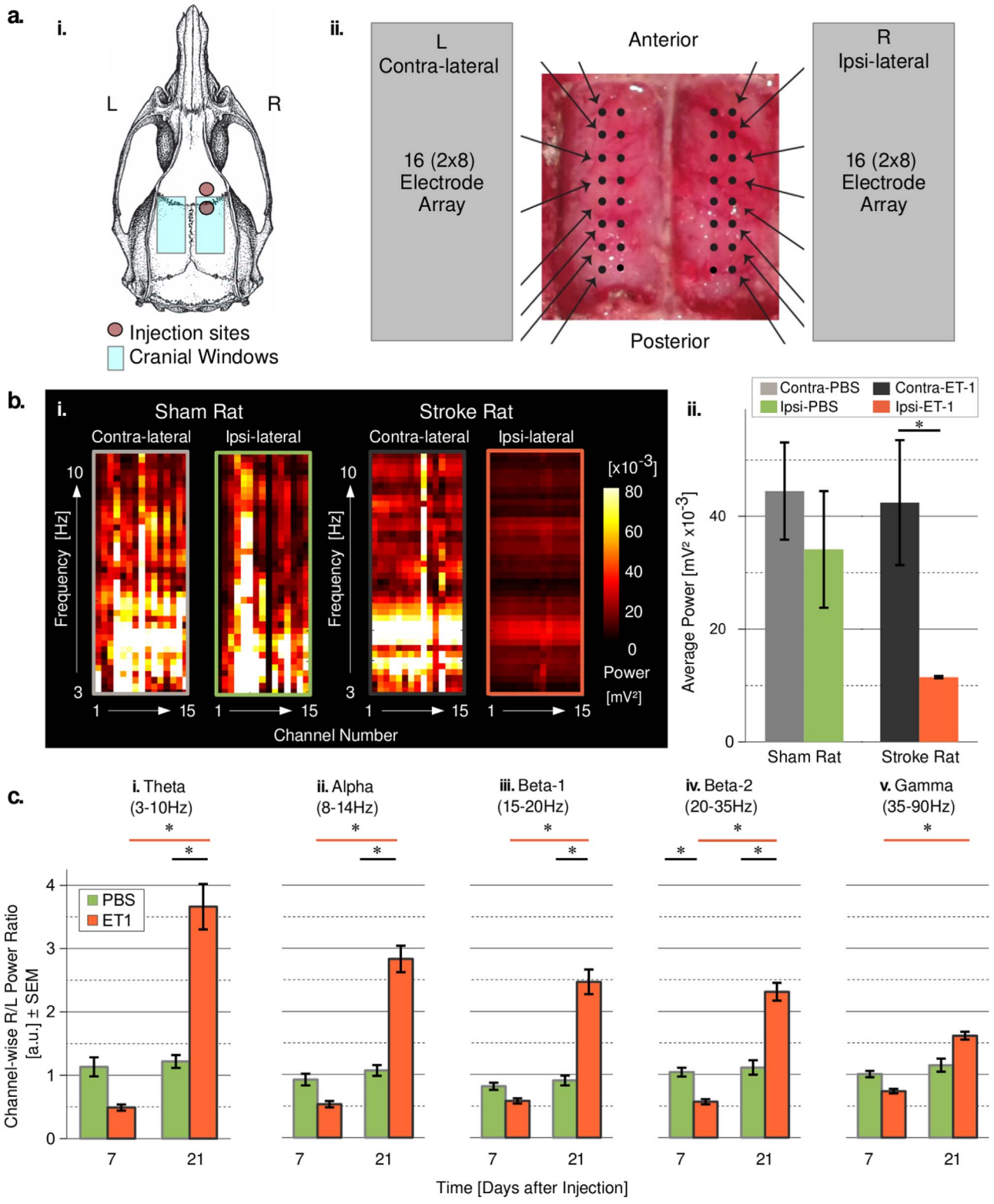

Fig. 2. Intra-cranial electrophysiological recordings of evoked responses. (a) A schematic of the surgical preparation for intracortical electrophysiological recordings, with the extent of cranial windows outlined in (a.i.) by blue rectangles. The injection sites made on day 0 for ET-1 or PBS (sham) injections are indicated by black outlined circles with red centres (a.i.). A photograph of a double cranial window preparation from a stroke rat seven days after stroke is shown in (a.ii.). The approximate placement of the MEAs is indicated by grey rectangles, with electrodes shown as black circles. (b.i.) Recordings of spontaneous activity in Theta band from contra- and ipsi-lateral hemispheres of a representative sham and representative stroke rat on day seven. The corresponding average Theta band power across all channels from these two animals is shown in (b.ii.). (c) Inter-hemispheric channel-wise power ratios (sham in green; stroke in orange) averaged across channels, in each band, on days seven and 21 following stroke. Compared to sham animals, stroke rats exhibited decreased ipsilesional Beta-2 power on day seven ($P=0.03$); but increased ipsilesional power in all bands (with the exception of Gamma) on day 21 ($P < 0.03$). The average inter-hemispheric power ratio in stroke rats increased between day seven and 21 in all frequency bands ($P < 0.008$). (For interpretation of the references to color in this figure legend, the reader is referred to the web version of this article.)

Table 1
Channel-wise ipsi- to contra-lateral spontaneous activity power ratios.

Band	Channel-wise ipsi- to contra-lateral power ratio [a.u.]			
	Sham animals		Stroke animals	
	Day 7 (N=5)	Day 21 (N=5)	Day 7 (N=5)	Day 21 (N=4)
Theta [3–10 Hz]	1.1 ± 0.2	1.2 ± 0.1	0.49 ± 0.05	3.7 ± 0.4 ** †
Alpha [8–14 Hz]	0.92 ± 0.09	1.06 ± 0.09	0.53 ± 0.05	2.8 ± 0.2 ** †
Beta-1 [15–20 Hz]	0.81 ± 0.06	0.91 ± 0.08	0.58 ± 0.04	2.5 ± 0.2 ** †
Beta-2 [20–35 Hz]	1.04 ± 0.07	1.1 ± 0.1	0.57 ± 0.04 *	2.3 ± 0.1 ** †
Gamma [35–90 Hz]	1.01 ± 0.05	1.1 ± 0.1	0.74 ± 0.04	1.61 ± 0.06 **

The channel-wise ipsi- to contra-lateral power ratios averaged across channels and across animals in the sham and stroke groups for each band of interest (± SEM) are reported at seven and 21 days after surgery. At seven days, stroke animals had a lower Beta-2 band inter-hemispheric ratio (* P=0.03) relative to sham animals. Inter-hemispheric ratios increased in every band in stroke animals between seven and 21 days (** P < 0.008). Further, between groups, the inter-hemispheric ratios in stroke animals was greater than in sham animals in all bands († P < 0.03) except Gamma [35–90 Hz] (P=0.08).

3.5. Resting perfusion and perfusion responses to hypercapnia

CASL MRI experiments were performed to estimate resting perfusion and reactivity to hypercapnic challenges, at seven and 21 days after stroke or sham-surgery. The ipsilateral ROI signal was normalized to the contralateral ROI signal to facilitate comparisons across groups and time. CASL maps overlaid on structural T_2-weighted MR-images from representative stroke and sham animals at seven and 21 days after surgery are shown in Fig. 4, with resting perfusion shown in Fig. 4(a). Sham animals showed no lateralization in resting perfusion either seven (0.96 ± 0.01) or 21 days (0.92 ± 0.02) post-surgery. In contrast, stroke animals exhibited resting perfusion lateralization at day seven (1.63 ± 0.08), but not at day 21 (0.96 ± 0.07). In particular, ipsilateral resting perfusion was elevated (relative to contralateral levels) in stroke animals compared to sham-operated animals at seven days (P=0.00001), but not at 21 days (P=0.7). Further, ipsi- relative to contra-lateral perfusion decreased with time in stroke animals (P=0.00001), but did not change in sham-operated animals (P=0.1). Contralateral resting perfusion of either group did not differ from that of healthy grey matter either seven days (with contralateral to whole brain non-lesioned gray matter perfusion ratio of 0.92 ± 0.03 in stroke and 0.98 ± 0.02 in sham-operated rats) or 21 days post-surgery (0.91 ± 0.03 in stroke and 0.98 ± 0.02 in sham-operated rats). Furthermore, normalized contralateral resting perfusion did not change with time in either group (P=0.6).

Reactivity to hypercapnia at seven and 21 days after surgery is shown in Fig. 4(b). As with resting perfusion, sham animals exhibited no lateralization in perfusion responses on day seven: 1.1 ± 0.2; or on day 21: 1.2 ± 0.1. In contrast, stroke rats showed elevated ipsi- relative to contra-lateral vascular reactivity at day seven: 1.8 ± 0.2 and 21: 2.1 ± 0.3 post-stroke. Perfusion response lateralization did not change with time in either group (sham: P=0.7; stroke: P=0.4). Ipsilesional perfusion responses were elevated (relative to contralaterally) in stroke animals compared to sham-operated animals at both seven (P=0.04) and 21 days (P=0.03). Contralateral perfusion responses were not different from those in healthy grey matter in either group either seven days (with contralateral to whole brain non-lesioned gray matter perfusion response ratio of 0.9 ± 0.1 in stroke and 0.9 ± 0.1 in sham-operated rats), or 21 days (0.89 ± 0.06 in stroke and 0.95 ± 0.08 in sham-operated rats) post-surgery. Furthermore, contralateral perfusion responses did not change with time in either group (P=0.6).

3.6. Inflammatory cell, neuronal and vascular changes in the ipsilesional cortex

Serial coronal sections were prepared with GFAP (astrocytes), Iba-1 (microglia/macrophage), NeuN (neurons) and RECA-1 (endothelial cells) immunofluorescent stains. The number of sections included in these analyses are summarized in Supplementary Table 5. GFAP showed widespread astrocytic activation within the ipsilesional hemisphere, with a pronounced increase in the astrocytic activation in the perilesional cortex. Dense clusters of active astrocytes were also present in the caudate putamen, piriform cortex, and olfactory tubercle. These ROIs were chosen by visual inspection of GFAP and Iba-1 stained sections. The ipsi- to contra-lateral signal ratio for each of the ROIs for the aforementioned immunofluorescent stains in both groups (stroke and sham) at day seven and 21 are shown in Fig. 5a (GFAP) and b (Iba-1) and Fig. 6a (NeuN) and b (RECA-1).

At both time points, ipsi- (relative to contra-lesional) GFAP and Iba-1 signal intensity was elevated in all ROIs in the stroke vs. sham

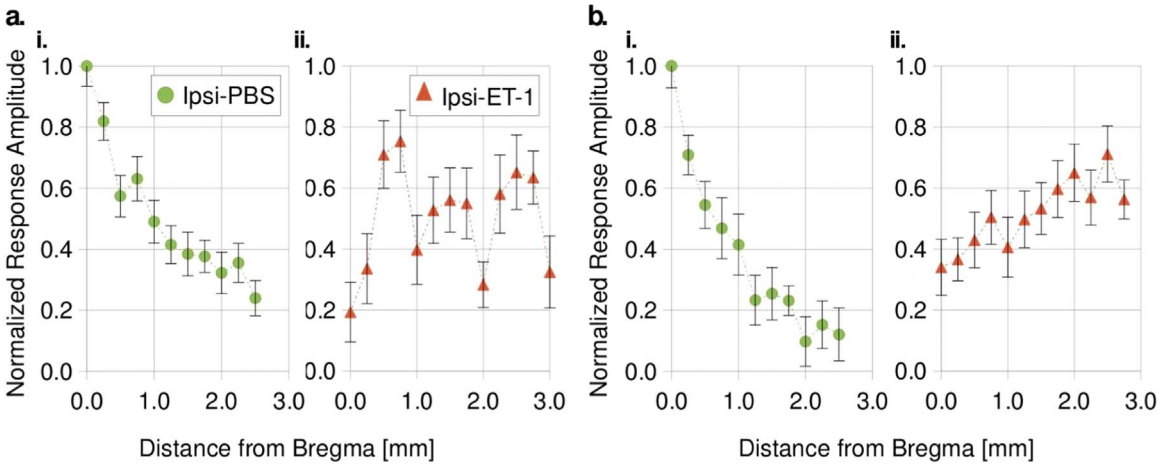

Fig. 3. Intra-cranial electrophysiological recordings of spontaneous activity. Left-to-right normalized LFP responses to bilateral forepaw stimulation, averaged across all animals, as a function of distance from Bregma: (a.) day seven: sham group (i.) and stroke group (ii.). (b.); day 21: sham group (i.) and stroke group (ii.). In sham animals, LFP amplitude decreased with distance from Bregma seven and 21 days after surgery, with no dependence of LFP amplitude on time after injection. Ipsilateral LFP responses in stroke animals were different than those in control animals at both time points (P < 0.0001). Ipsilesionally there was no dependence of LFP amplitude on distance from Bregma on day seven following stroke. On day 21 after stroke, ipsilesional LFP response amplitude increased from Bregma to +3.0 mm in the A-P direction (P < 0.0001).

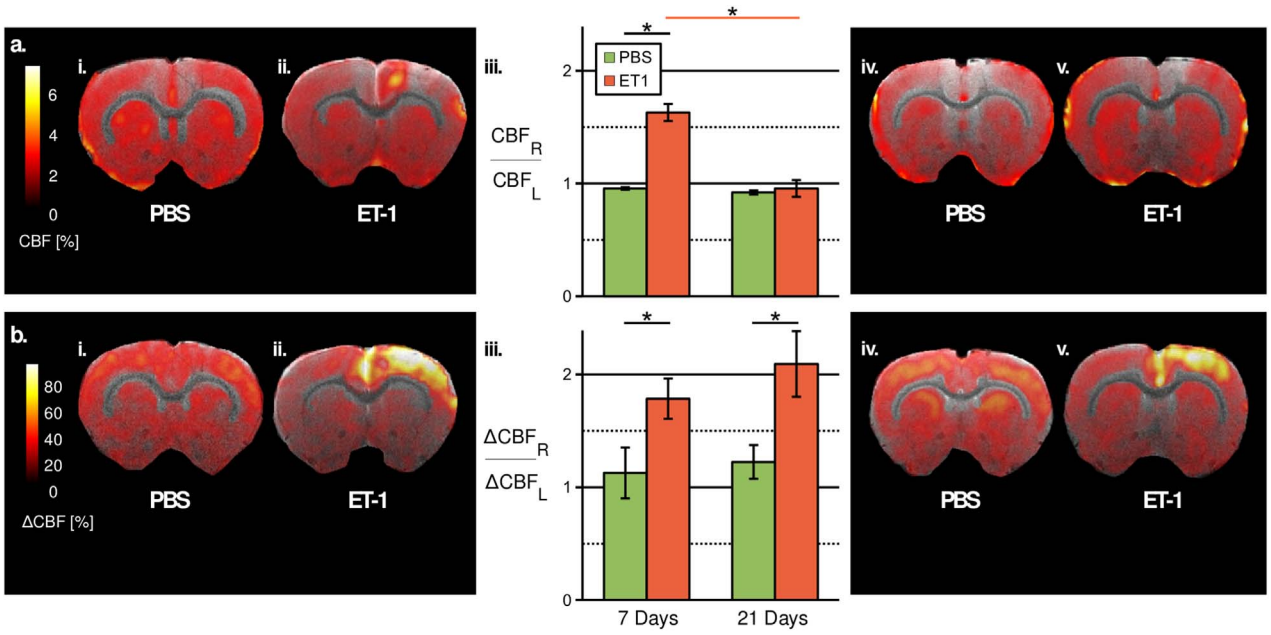

Fig. 4. Functional MRI of resting blood flow, and cerebrovascular reactivity to 10% CO_2. Fig. 4. Overlaid on T_2-weighted MRI is the resting perfusion (a) and blood flow response to 10% CO_2 (b) in representative animals (i, ii, iv, v). CASL data across all animals within each group are shown in (iii). Unlike sham rats, stroke rats exhibited lateralization in baseline perfusion and vascular reactivity. In particular, stroke rats showed ipsilesional hyperperfusion (at 1.63 ± 0.08 fold contralesional levels) and hyperreactivity (at 1.8 ± 0.2 fold contralesional levels) on day seven. By 21 days following ischemic insult, baseline perfusion of stroke rats was no longer lateralized ($P < 0.0001$), yet ipsilesional vascular reactivity remained elevated (at 2.1 ± 0.3 fold contralesional levels). There was no lateralization of either resting perfusion or perfusion response to hypercapnia in sham animals at either time point.

group. Table 2 summarizes the ipsi- to contra-lateral signal intensity ratios for both time points for each ROI. There was a time-dependent increase in the inter-hemispheric ratio of GFAP signal in stroke animals in all ROIs except for the piriform cortex between day seven and 21, indicating progressive astrocytic activation (see Fig. 5a). Conversely, there was no change in the ipsi- to contra-lesional signal intensity ratio of Iba-1 from stroke animals between day seven and 21, indicating no change in microglia/macrophage recruitment and activation over this period (see Fig. 5b). Sham animals showed no lateralization of GFAP or Iba-1 signals at either time point.

On day seven post surgery, the ipsi- to contra-lesional ratio of NeuN signal was lower in stroke animals compared to shams: 0.35 ± 0.05 (stroke rats) vs. 1.03 ± 0.04 (sham animals) ($P < 0.0001$). Neuronal loss was also observed in the caudate putamen: 0.32 ± 0.07 (stroke) vs. 0.96 ± 0.08 (sham) ($P=0.0004$), and piriform cortex: 0.5 ± 0.2 (stroke) vs. 0.96 ± 0.04 (sham) ($P=0.004$). Neuronal loss thus extended to regions distal from the site of injection. The decrease in neuronal density persisted on day 21 in the cortex 0.36 ± 0.06 (stroke) vs. 0.97 ± 0.05 (sham) ($P < 0.0001$) and caudate putamen 0.10 ± 9 (stroke) vs. 0.9 ± 0.1 (sham) ($P=0.007$).

The RECA-1 ipsi- to contra-lateral cortical signal ratio was elevated in stroke animals compared to that of sham animals at both time points, indicating peri-lesional angiogenesis on day seven: 1.6 ± 0.1 (stroke) vs. 1.00 ± 0.04 (sham), ($P=0.0001$); and 21: 2.7 ± 0.4 (stroke) vs. 1.02 ± 0.04 (sham) ($P < 0.0001$). Further, this ratio rose with time in stroke animals ($P=0.002$) indicating progressive morphological remodelling of the micro-vasculature in the peri-lesional tissue (see Fig. 6b). No changes were observed in the caudate putamen, piriform cortex or olfactory tubercle. Fig. 7 summarizes the pathological findings for a representative stroke animal at seven days.

4. Discussion

The present work provided a multimodal characterization of the evolution of neurogliovascular function in the subacute stage of the focal ischemic injury. Over three weeks following ischemic insult, ET-1 micro-injection produced a stable lesion volume (~100 mm^3 or ~20% of the total brain volume), and a persistent impairment of left forelimb skilled reaching ability. Blood vessel density was increased ipsi- *vs.* contra-laterally and neuronal loss and inflammation were widespread. A week following stroke, resting perfusion and vascular reactivity to 10% CO_2 in ipsilesional cortices were elevated by 60% and 80% relative to corresponding levels contralesionally. Further, the topological pattern of LFP response amplitudes to bilateral forepaw stimulation were abolished and the average spontaneous neuronal activity attenuated by ~50%. Three weeks after stroke, ipsilesional hyperperfusion pseudo-normalized; while vascular reactivity remained at double the contralesional level. LFP evoked response amplitudes progressively increased with distance from the site of injury and the average ipsilesional spontaneous neuronal activity was twice that observed contralesionally.

4.1. Resting perfusion and perfusion responses to hypercapnia

The transient hyperperfusion and persistent hyperreactivity observed in the ipsilesional cortex in this work are consistent with a number of prior studies in rat MCAO models (Lin et al., 2008; Wang et al., 2002; Martin et al., 2012; Wegener et al., 2006). Two or four days following transient MCAO, rats are hyperperfused (Wang et al., 2002) and hyperperfusion persists between four and seven days following two-hour intra-luminal MCAO, with peri-lesional perfusion being double that of sham-operated rats at seven days (Martin et al., 2012), in excellent agreement with present findings. In a 60-minute MCAO model, Wegener et al. (2006) identified three outcome patterns dependent on lesion size and location, including limited hyperperfusion on day one, maximal hyperperfusion on day four, and decreased vaso-reactivity on day four but elevated on day 14, which is consistent with the present observations. The doubling of resting perfusion at seven days in the current study also falls within the reported range of ischaemia-induced ipsi- vs. contra-lesional perfusion elevation: 120-200% reported previously (van Lookeren et al., 1999; Wang et al., 2002; Martin et al., 2012).

In contrast, Shen et al. (2011) report hyperperfusion at 48 hrs to resolve by seven days, but also show perfusion changes strongly

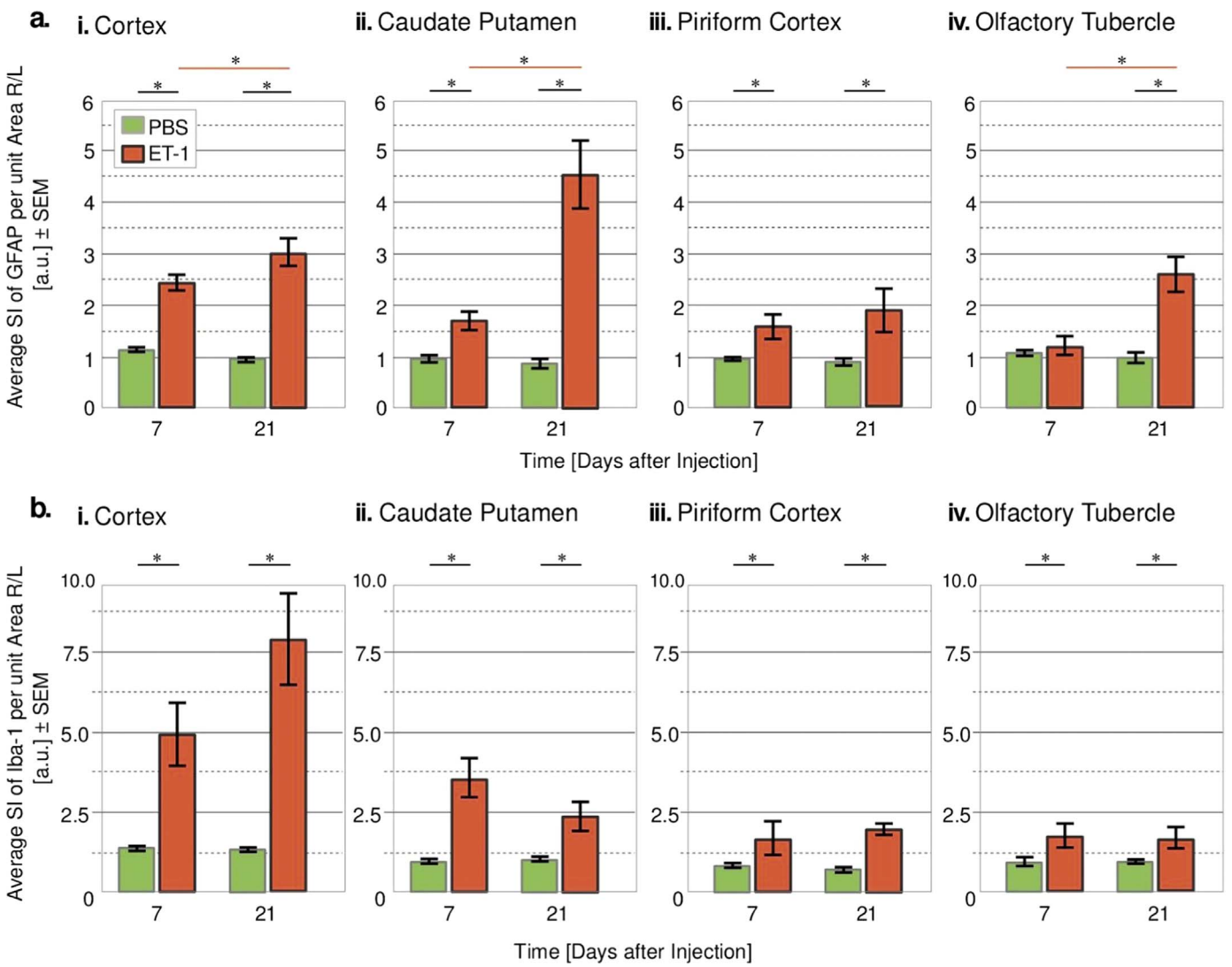

Fig. 5. GFAP and Iba-1 immunofluorescence. Interhemispheric ratio of GFAP (a) and Iba-1 (b) signal intensity per unit area averaged across all animals on days seven and 21 in the cortex (i), caudate putamen (ii), piriform cortex (iii), and olfactory tubercle (iv). On day seven and 21, stroke rats showed increased ipsilesional GFAP and Iba-1 signal in all ROIs, with the exception of GFAP in the olfactory tubercle on day seven. GFAP interhemispheric asymmetry increased between day seven and 21 in stroke rats in all ROIs expect for the piriform cortex.

dependent on MCAO duration. In addition, Shen and colleagues observe *decreased* perilesional perfusion responses to hypercapnia concomitant to increased resting perfusion at 48 hrs post stroke. Due to the highly dynamic changes in the perilesional vascular function during the first week following stroke (Wegener et al., 2006), it is hard to relate the vasoreactivity at seven days (our first post-stroke sampling point) to a measurement at 48 hrs. As with prior hemodynamic studies on ischemic injury progression (Heiss et al., 1997; Shen et al., 2011; Hayward et al., 2011; Wegener et al., 2013), the current CASL protocol was limited in that only relative measures of cortical hemodynamics were made. Within-subject measurements of T_1 relaxation time, inversion efficiency, and sampling at a series of post-labelling intervals should be undertaken in future studies to allow absolute perfusion quantification, following optimization of these sequences to minimize total scan time and thus curb attrition. Moreover, propofol anaesthesia, employed in the current study during all MRI experiments, induces 20–60% regional vasoconstriction (Cenic et al., 2000; Werner et al., 1993), likely due to reduced metabolic demand (Werner et al., 1993; Dam et al., 1990). Although logistically complex, modifications to the present protocol to enable imaging in awake animals could be used to evaluate possible interactions between the effects of ischaemia and propofol anaesthesia.

4.2. Injury induced angiogenesis

Ischaemia-induced angiogenesis has been previously reported (Hayward et al., 2011; Wegener et al., 2013) and likely underlies the elevated peri-lesional resting perfusion observed in the present work. Between two and seven days following MCAO, Martin et al. (2012) show an increase in endothelial cell ($CD31^+$) number perilesionally between two and seven days following MCAO. Also in an MCAO model, Wegener et al. (2006) and Hayward et al. (2011), show perilesional RECA-1 staining at 140% the contralesional level two (Wegener et al., 2013) and 12 weeks (Hayward et al. 2011) post-stroke. Furthermore, tripling of micro-vascular density following stroke was seen by Lin et al. (2008) 14–21 days post-MCAO, who suggested it resulted from a delayed surge of angiogenesis. The presently observed increase in endothelial cell density in the ipsilesional cortex is thus in excellent agreement with prior studies.

However, although perilesional vascular density remained elevated at 21 days, resting perfusion normalized. Pruning, recruitment of mural cells, the generation of an extracellular matrix, specialization of the vessel wall, and the functional integration of nascent vasculature are highly dependent on the spatio-temporal interaction of new micro-vessels and the surrounding neurons and glia (cf. Review by Korn and

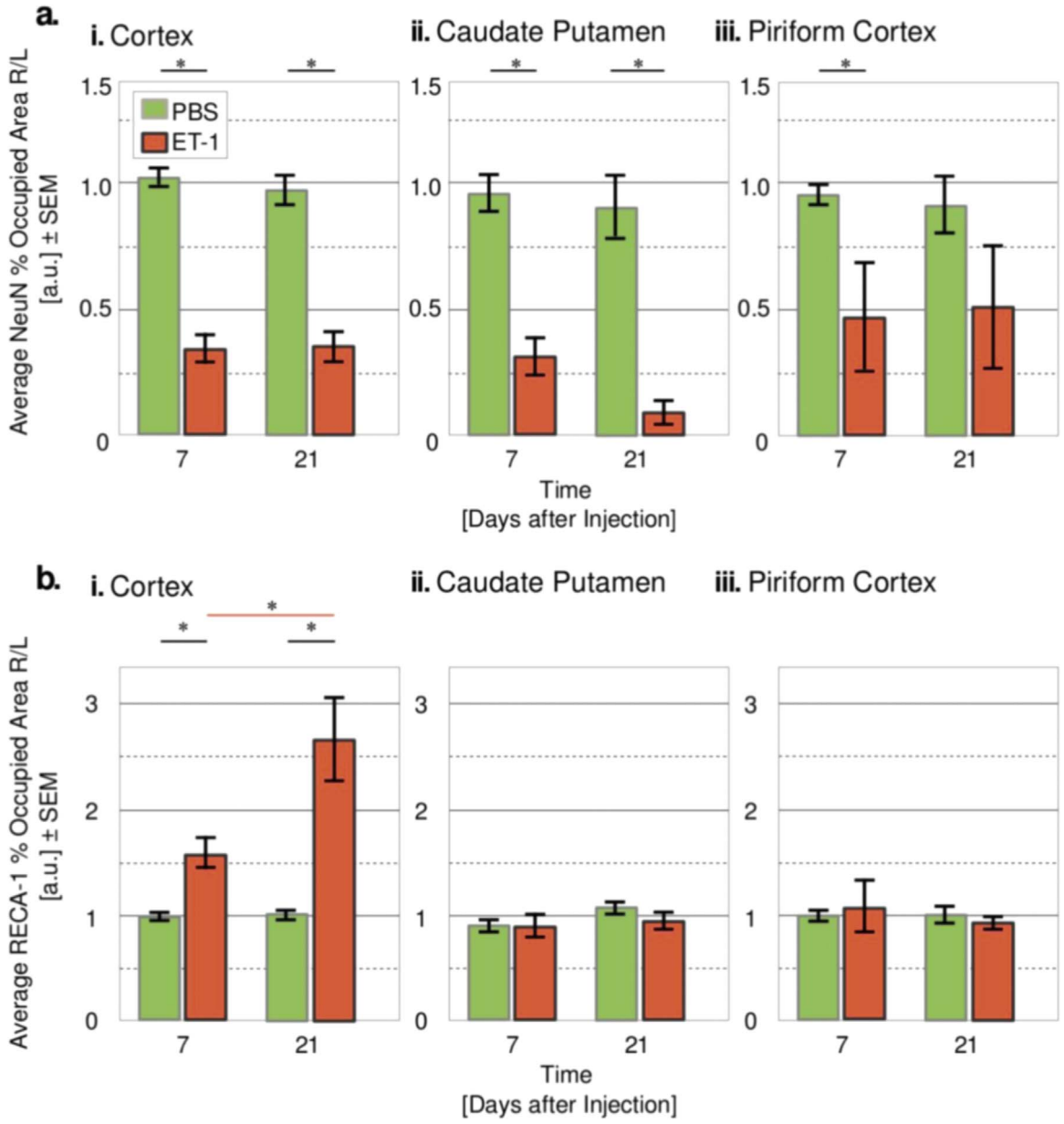

Fig. 6. NeuN and RECA-1 immunofluorescence. Interhemispheric ratio of percent area occupied by positively stained NeuN (a) and RECA-1 (b) cells on day seven and 21 in the cortex (i), caudate putamen (ii), and piriform cortex (iii). Stroke rats exhibited neuronal loss on both day seven and 21 in all ROIs, with the exception of the piriform cortex on day 21. There were no time-dependent changes in NeuN staining in either cohort. Stroke animals showed increased endothelial cell density (on RECA-1) ipsilesionally on day seven that increased further over the next two weeks. (* P≤0.01).

Augustin (2015)). Perilesional neuronal loss may have led to extensive pruning of new vessels and hence unperfused vessels by day 21 (Korn and Augustin 2015). Indeed, by 13 weeks following transient MCAO, peri-lesional micro-vessel density (doubled at four weeks) regresses to contralesional levels (Yu et al., 2007). Furthermore, perilesional hyperreactivity to hypercapnia may have resulted from lower resistance of newly added, immature vessels (White and Bloor, 1992).

4.3. Remapping of cortical somatotopy following focal ischaemia

Electrophysiological recordings show a somatotopic organization of the primary somatosensory cortex in the healthy rat brain (Hosp et al., 2008). Accordingly, we observed monotonically decreasing forepaw stimulation elicited LFP response amplitudes contralaterally in both groups and ipsilaterally in the sham group. One day following transient MCAO, disruption of motor-evoked potentials ipsilesionally has been observed and is thought to result from persistent transmission failure of cortical synapses, which likely contributes to motor dysfunction (Bolay and Dalkara, 1998). In the present work, no evidence of a spatial pattern in ipsilesional LFP response amplitudes was observed a week following stroke.

Somatosensory LFP responses to forepaw stimulation improve one week following ischemic damage to the striatum and fully recover by four weeks (Shih et al., 2014). Thus, distal to the site of injury, LFP responses are compromised transiently following stroke, but can recover to be indistinguishable from those in controls (Shih et al., 2014). In the present work, we observed a new topological pattern to emerge by three weeks: evoked potential amplitudes increased monotonically with distance from the site of injury. The present findings hence likely represent recovery of function in the lesion periphery (Shih et al., 2014), and possibly remapping.

Following an ischemic injury, sensory and motor function performed by injured tissue prior to infarction has the potential to remap to contra- and peri-lesional areas. In general, remapping manifests as

Table 2
Ipsi- to contra-lateral ratios of optical density from immunofluorescence analysis.

Stain	ROI	Ipsi- to Contra-lateral Fluorescence [a.u.]			
		Control Group		Ischemic Group	
		Day 7	Day 21	Day 7	Day 21
GFAP	*i. Cortex*	1.15 ± 0.04	0.98 ± 0.03	2.5 ± 0.1 ‡	3.0 ± 0.3 ‡
	ii. Caudate Putamen	0.98 ± 0.07	0.87 ± 0.1	1.7 ± 0.2 †	4.6 ± 0.7 †
	iii. Piriform Cortex	0.96 ± 0.05	0.91 ± 0.08	1.6 ± 0.2 *	1.9 ± 0.4 **
	iv. Olfactory Tubercle	1.08 ± 0.05	0.99 ± 0.08	1.2 ± 0.2 **	2.6 ± 0.3 ‡
Iba-1	*i. Cortex*	1.08 ± 0.04	1.07 ± 0.04	3.8 ± 0.5 ‡	4.6 ± 0.8 ‡
	ii. Caudate Putamen	0.99 ± 0.06	1.05 ± 0.06	3.6 ± 0.6 †	2.4 ± 0.5 **
	iii. Piriform Cortex	0.89 ± 0.04	0.77 ± 0.04	1.71 ± 0.5 **	2.0 ± 0.2 ‡
	iv. Olfactory Tubercle	0.97 ± 0.1	0.99 ± 0.07	1.80 ± 0.4 *	1.7 ± 0.4 *
RECA-1	*i. Cortex*	1.00 ± 0.04	1.02 ± 0.04	1.6 ± 0.1 ‡	2.7 ± 0.4 ‡
	ii. Caudate Putamen	0.91 ± 0.06	1.08 ± 0.05	0.9 ± 0.1	0.96 ± 0.08
	iii. Piriform Cortex	1.01 ± 0.05	1.01 ± 0.08	1.0 ± 0.3	0.94 ± 0.06
NeuN	*i. Cortex*	1.03 ± 0.04	0.97 ± 0.05	0.35 ± 0.05 ‡	0.36 ± 0.06 ‡
	ii. Caudate Putamen	0.96 ± 0.08	0.9 ± 0.1	0.32 ± 0.07 †	0.10 ± 0.04 **
	iii. Piriform Cortex	0.96 ± 0.04	0.9 ± 0.1	0.5 ± 0.2 **	0.5 ± 0.2

The average ipsi- to contra-lateral signal intensity (GFAP and Iba-1) or relative area (RECA-1 and NeuN) across all animals at seven and 21 days after surgery. In comparison to sham rats, stroke animals showed increased ipsilesional astrogliosis (GFAP) and macrophage/microglia recruitment in all ROIs. Angiogenesis was observed only in the perilesional cortical tissue, while neuronal loss was evident in all ROIs except for the olfactory tubercle. * $P < 0.05$, ** $P < 0.01$, † $P < 0.001$, ‡ $P < 0.0001$.

gross physiological changes in the responsiveness of neuronal networks demonstrating widespread functional plasticity during the weeks-months following stroke (Murphy and Corbett, 2009; Carmichael, 2012). Although studies have provided evidence of remapping during the chronic phase of ischemic injury progression, what the features of the remapped response (magnitude, kinetics, or spatial pattern) imply for functional outcome is still controversial (Buma et al., 2010; Buetefisch, 2015). In the present work, neurophysiological changes

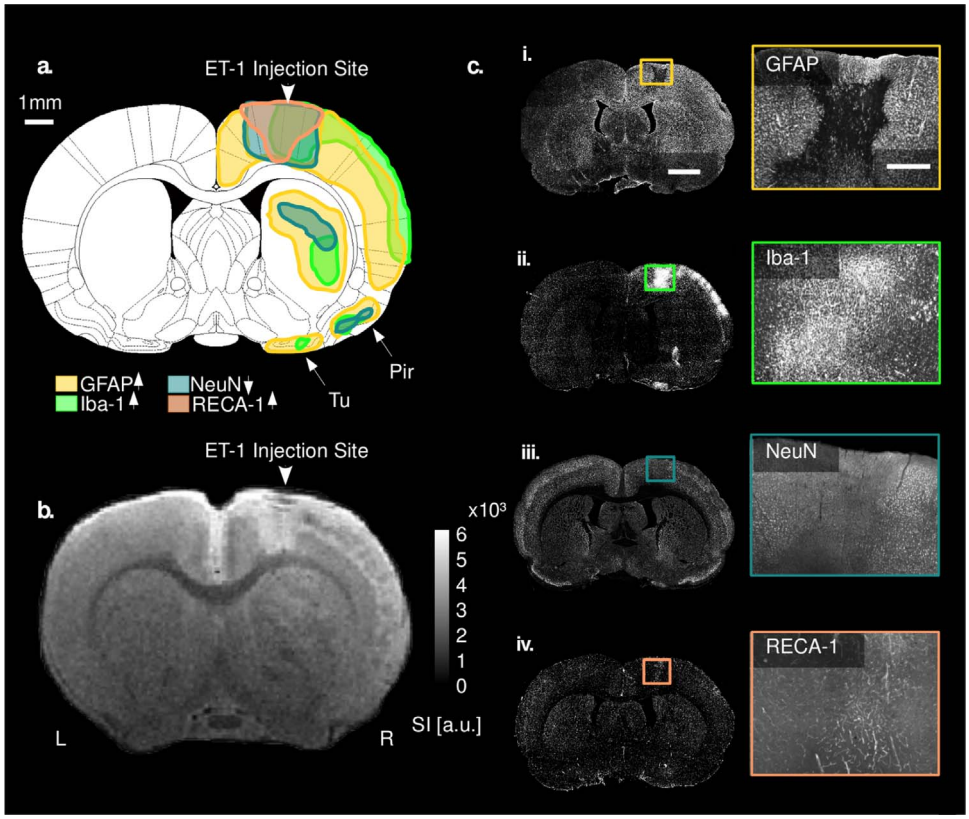

Fig. 7. Immunofluorescence in a representative subject and corresponding T_2 -weighted MRI. Fig. 7(a) Atlas drawing (Paxinos and Watson, 2005) at –0.36 mm A-P from Bregma, hence proximal to the posterior site of ET-1 injection, with an overlay summarizing the immunohistochemical changes observed in stroke animals (scale bar: 1 mm). Coloured regions indicate areas of astrocytic activation (yellow), microglia/macrophage recruitment (green), decreased neuronal density (blue), and increased vascular density (peach). b. T_2-weighted slice roughly corresponding to the atlas section in (a) acquired in a representative rat seven days post-stroke. (c.) Example coronal sections from rat in (b) at -0.36 mm from Bregma (scale bar: 1 mm) and insets showing the region surrounding the ET-1 injection site (i. GFAP ii. Iba-1 iii. NeuN iv. RECA-1). Scale bar: 500 μm. Pir: piriform cortex; Tu: olfactory tubercle. (For interpretation of the references to color in this figure legend, the reader is referred to the web version of this article.)

were not accompanied by improvement of skilled reaching ability on the Montoya Staircase test, possibly as a result of the incomplete recovery process after three weeks. Furthermore, the Montoya staircase task is particularly resistant to spontaneous recovery (associated with cortical reorganization) (Murphy and Corbett, 2009). However, significant time-dependent performance improvement on skilled reaching tasks has been observed with frequent testing in animals with small stroke volumes (10–15 mm^3), and evidence of cortical remapping concomitant with behavioural performance improvement with intensive reach training therapy (Nishibe et al., 2015). Montoya staircase testing was employed in the present work because it is quantitative, not subject to experimenter bias (Murphy and Corbett, 2009), and reports on clinically relevant performance (upper limb impairment being the most common motor deficit in patients) (Kleim et al., 2007). Notwithstanding, a battery of behavioural tests should be used in future studies to assess overall functional gains over a longer observation period.

4.4. Changes in neuronal excitability following focal ischaemia

As further evidence of neuronal functional adaptation, a pronounced shift in the inter-hemispheric asymmetry of spontaneous neuronal activity was observed in ischemic animals between seven and 21 days after stroke. The ipsilesional cortex was hypoactive (by ~50% relative to contralesional levels) at day seven, yet became hyperactive by day 21 (at two fold contralesional levels). Magnetoencephalography in patients with partial motor recovery similarly show an increase in band power ipsi- relative to contra-lesionally (Tecchio et al., 2006). Relative hyperactivity is thought to result from increased intra-regional neuronal firing synchrony and, at a cellular level, an increase in intrinsic neuronal excitability (Tecchio et al., 2006).

Preclinically, Clarkson et al. (2010) reports elevated tonic inhibition (hypoexcitability) at one and two weeks following ischemic insult in a mouse photothrombotic model. Unlike the present study, Clarkson et al. (2010) do not observe evidence of delayed endogenous hyperexcitability. However, the latter assessment in Clarkson et al. (2010) was made at two weeks (*vs*. three weeks in the current work), which may have been too early for endogenous hyperexcitability to manifest. In addition, the photothrombotic model employed by Clarkson et al. (2010), produces a small necrotic core with no re-perfusion and very little perilesional tissue, which may have created a different ischemic micro-environment and subacute stage injury progression than the one produced by ET-1 injection in the present study. Notwithstanding, the success of treatment with an inverse agonist of GABA-A receptor by Clarkson et al., (2010) and in our earlier study (Lake et al., 2015) suggests that accelerating and/or potentiating delayed endogenous hyperexcitability (observed in the present work) may prove beneficial.

4.5. Widespread neuroinflammation

The delayed astrocytic activation accompanied by decreased neuronal density (> 50% decrease in NeuN staining) in the peri-lesional cortex observed in the present work are in accordance with earlier reports on the time course of inflammatory cell infiltration and neuronal cell death in the subacute phase of ischemic injury progression (Rossini et al., 2001; Nguemeni et al., 2015). It is noteworthy that the area of reduced neuronal density tightly circumscribed the site of injection and comprised a tissue volume of ~0.065 mm^3, thus being much smaller than the area to which electrode arrays were sensitive (~0.2 mm^3). Neuronal death was thus limited to the ischemic core, while neurons in the perilesional tissue exhibited time-dependent changes in activity, as evidenced on intracortical electrophysiology recordings.

Removed from the site of injury, a marked increase in astrocytic and microglia/macrophage activation was found in the ipsilesional caudate putamen, piriform cortex, and olfactory tubercle at both time points. Although each of these structures has been implicated in focal ischemic injury progression (namely astrogliosis in the olfactory tubercle, and neuroinflammation in the piriform cortex and caudate putamen); secondary ischemic injury effects in these brain regions are not commonly reported and their implications are unknown (Speliotes et al., 1995; Gualtieri et al., 2012). A key integrating structure, the olfactory tubercle is connected to both the piriform cortex (from which it receives monosynaptic olfactory input) and the caudate putamen (to which there are medium-sized dense-spine cell projections), which may explain why damage in these structures was observed (Fallon, 1983; Wesson and Wilson, 2011).

Although concomitant decreases in neuronal density in the caudate putamen and piriform cortex were found, there was no effect of stroke on neuronal density in the olfactory tubercle. Further, no regions distal to the site of injection showed changes in vascular density on immunohistochemistry; and no morphological or vascular functional changes were seen in any of these distal structures on MRI. The former suggests that angiogenesis may only accompany a supra-threshold degree of injury; whereas the latter is unsurprising given the limited sensitivity of structural MRI to subtle changes in tissue morphology. Finally, it is also possible that back-flow of ET-1 and its subsequent distribution through the subarachnoid space could have caused some distal injury.

5. Conclusion

On the whole, the present data demonstrated the complexity of the relationship between structure and function of brain neuronal and vascular networks, and emphasized the need for concomitant characterization of both over prolonged observation periods following ischemic insult. It is likely that the effects of cortical reorganization, via spatially-specific modulation of neurovascular function, on behavioural outcome critically depend on the timing and extent of such changes. The current findings warrant further exploration of neuronal activity patterns, vascular remodelling and neuroinflammation during the subacute stage of ischemic injury progression and the effects their modulation may have on long-term neurophysiological measures and behavioural outcome. As the vast majority of patients arrive at a care facility well outside of the hyperacute window, identifying ways through which outcome can be improved during the subacute and chronic stages is of utmost importance.

Funding acknowledgement

Funding support was received from the Canadian Institute for Health Research (#MOP 123411 and 264623). Funders played no further role in the present work than granting the means to conduct experiments.

Competing financial interests statements

None of the authors have any competing financial interests to disclose.

Appendix A. Supplementary material

Supplementary data associated with this article can be found in the online version at http://dx.doi.org/10.1016/j.neuroimage.2016.09.016.

References

Biernaskie, J., Corbett, D., Peeling, J., Wells, J., Lei, H., 2001. A serial MR study of cerebral blood flow changes and lesion development following endothelin-1-induced ischemia in rats. Magn. Reson. Med. 46, 827–830. http://dx.doi.org/10.1002/mrm.1263.

Bolay, H., Dalkara, T., 1998. Mechanisms of motor dysfunction after transient MCA occlusion: persistent transmission failure in cortical synapses is a major determinant. Stroke 29, 1988–1993. http://dx.doi.org/10.1161/01.STR.29.9.1988.
Buetefisch, C.M., 2015. Role of the contralesional hemisphere in post-stroke recovery of upper extremity motor function. Front. Neurol. 6, 214. http://dx.doi.org/10.3389/fneur.2015.00214.
Buma, F.E., Lindeman, E., Ramsey, N.F., Kwakkel, G., 2010. Functional neuroimaging studies of early upper limb recovery after stroke: a systematic review of the literature. Neurorehabil. Neural Repair. 24, 589–608. http://dx.doi.org/10.1177/1545968310364058.
Carmichael, S.T., 2005. Rodent models of focal stroke: size, mechanism and purpose. NeuroRx 2, 396–409. http://dx.doi.org/10.1602/neurorx.2.3.396.
Carmichael, S.T., 2012. Brain excitability in stroke: the yin and yang of stroke progression. Arch. Neurol. 69, 161–167. http://dx.doi.org/10.1001/archneurol.2011.1175.
Chang, C.H., Chen, C.C., Siow, T.Y., Hsu, S.H., Hsu, Y.H., Jaw, F.S., Chang, C., 2013. High resolution structural and functional assessments of cerebral microvasculature using 3D Gas delta-R2*-mMRA. PLoS One 8, 1–10. http://dx.doi.org/10.1371/journal.pone.0078186.
Clarkson, A.N., Huang, B.S., MacIsaac, S.E., Mody, I., Carmichael, T.S., 2010. Reducing excessive GABAergic tonic inhibition promotes post-stroke functional recovery. Nature 468, 305–309. http://dx.doi.org/10.1038/nature09511.
Cox, R.W., 1996. AFNI: software for analysis and visualization of functional magnetic resonance neuroimages. Comput. Biomed. Res. 29, 162–173. http://dx.doi.org/10.1006/cbmr.1996.0014.
Dijkhuizen, R.M., Singhal, A.B., Mandeville, J.B., Wu, O., Halpern, E.F., Finklestein, S.P., Rosen, B.R., Lo, E.H., 2003. Correlation between brain reorganization, ischemic damage, and neurologic status after transient focal cerebral ischemia in rats: a functional magnetic resonance imaging study. J. Neurosci. 23, 510–517.
Fallon, J.H., 1983. The islands of Calleja complex of rat basal forebrain II: connections of medium and largesized cells. Brain Resb. Bull. 10, 775–793. http://dx.doi.org/10.1016/0361-9230(83)90210-1.
Griffin, K.M., Blau, C.W., Kelly, M.E., O'Herlihy, C., O'Connell, P.R., Jones, J.F., Kerskens, C.M., 2010. Propofol allows precise quantitative arterial spin labelling functional magnetic resonance imaging in the rat. Neuroimage 51 (4), 1395–1404. http://dx.doi.org/10.1016/j.neuroimage.2010.03.024.
Gualtieri, F., Curia, G., Marinelli, C., Biagini, G., 2012. Increased perivascular laminin redicts damage to astrocytes in CA3 and piriform cortex following chemoconvulsive treatments. Neuroscience 218, 278–294. http://dx.doi.org/10.1016/j.neuroscience.2012.05.01.
Hallett, M., 2001. Plasticity of the human motor cortex and recovery from stroke. Brain Res. Brain Res. Rev. 36, 169–174. http://dx.doi.org/10.1016/S0165-0173(01)00092-3.
Hast, A., 2014. Simple filter design for first and second order derivatives by a double filtering approach. Pattern Recognit. Lett. 42, 65–71. http://dx.doi.org/10.1016/j.patrec.2014.01.014.
Hayward, N.M., Yanev, P., Haapasalo, A., Miettinen, R., Hiltunen, M., Gröhn, O., Jolkkonen, J., 2011. Chronic hyper-perfusion and angiogenesis follow subacute hypoperfusion in the thalamus of rats with focal cerebral ischemia. J. Cereb. Blood Flow Metab. 21, 1119–1132. http://dx.doi.org/10.1038/jcbfm.2010.202.
Heiss, W.D., Graf, R., Löttgen, J., Ohta, K., Fujita, T., Wagner, R., Grond, M., Weinhard, K., 1997. Repeat positron emission tomographic studies in transient middle cerebral artery occlusion in cats: residual perfusion and efficacy of postischemic reperfusion. J. Cereb. Blood Flow Metab. 17, 388–400. http://dx.doi.org/10.1097/00004647-199704000-00004.
Hosp, J.A., Molina-Luna, K., Hertler, B., Atiemo, C.O., Stett, A., Luft, A.R., 2008. Thin-film epidural microelectrode arrays for somatosensory and motor cortex mapping in rat. J. Neurosci. Methods 172, 255–262. http://dx.doi.org/10.1016/j.jneumeth.2008.05.010.
ImageMagick Studio LLC, 2013. Non-Profit Organization Dedicated to Making Software Imaging Solutions Freely Available. Copyright 1999-2013 ⟨http://www.imagemagick.org/script/index.php⟩.
Jiang, Q., Zhang, Z.G., Ding, G.L., Silver, B., Zhang, L., Meng, H., Lu, M., Pourabdillah-Nejed-D, S., Wang, L., Savant-Bhonsale, S., Li, L., Bagher-Ebadian, H., Hu, J., Arbab, A.S., Vanguri, P., Ewing, J.R., Ledbetter, K.A., Chopp, M., 2006. MRI detects white matter reorganization after neural progenitor cell treatment of stroke. NeuroImage 32, 1080–1089. http://dx.doi.org/10.1016/j.neuroimage.2006.05.025.
Kang, J.K., Bénar, C., Al-Asmi, A., Khani, Y.A., Pike, G.B., Dubeau, F., Gotman, J., 2003. Using patient-specific hemodynamic response functions in combined EEG-fMRI studies in epilepsy. Neuroimage 20, 1162–1170. http://dx.doi.org/10.1016/S1053-8119(03)00290-8.
Kidwell, C.S., Alger, J.R., Saver, J.L., 2003. Beyond mismatch: evolving paradigms in imaging the ischemic penumbra with multimodal magnetic resonance imaging. Stroke 34, 2729–2735. http://dx.doi.org/10.1161/01.STR.0000097608.38779.CC.
Kleim, J.A., Boychuk, J.A., Adkins, D.L., 2007. Rat models of upper extremity impairment in stroke. ILAR J. 48, 374–834. http://dx.doi.org/10.1093/ilar.48.4.374.
Korn, C., Augustin, H.G., 2015. Mechanisms of vessel pruning and regression. Dev. Cell. 34, 5–17. http://dx.doi.org/10.1016/j.devcel.2015.06.004.
Krishnamurthi, R.V., Feigin, V.L., Forouzanfar, M.H., Mensah, G.A., Connor, M., Bennett, D.A., Moran, A.E., Sacco, R.L., Anderson, L.M., Truelsen, T., O'Donnell, M., Venketasubramanian, N., Barker-Collo, S., Lawes, C.M., Wang, W., Shinohara, Y., Witt, E., Ezzati, M., Naghavi, M., Murray, C., 2013. Global Burden of Diseases, Injuries, Risk Factors Study 2010 (GBD 2010); GBD Stroke Experts Group. Global and regional burden of first-ever ischaemic and haemorrhagic stroke during 1990-2010: findings from the Global Burden of Disease Study 2010. Lancet Gob. Health 1, 259–281. http://dx.doi.org/10.1016/S2214-109X(13)70089-5.
Krupiński, J., Kałuza, J., Kumar, P., Kumar, S., Wang, J.M., 1992. Some remarks on the growth-rate and angiogenesis of microvessels in ischemic stroke. Morphometric and immunocytochemical studies. Patol. Pol. 44, 203–209.
Krupiński, J., Kałuza, J., Kumar, P., Kumar, S., Wang, J.M., 1994. Role of angiogenesis in patients with cerebral ischemic stroke. Stroke 25, 1794–1798. http://dx.doi.org/10.1161/01.STR.25.9.1794.
Laird, N.M., Ware, J.H., 1982. Random-effects models for longitudinal data. Biometrics 38, 963–974. http://dx.doi.org/10.1007/978-3-642-11760-22.
Lake, E.M., Chaudhuri, J., Thomason, L., Janik, R., Ganguly, M., Brown, M., McLaurin, J., Corbett, D., Stanisz, G.J., Stefanovic, B., 2015. The effects of delayed reduction of tonic inhibition on ischemic lesion and sensorimotor function. J. Cereb. Blood Flow. Metab. 35, 1601–1609. http://dx.doi.org/10.1038/jcbfm.2015.86.
Lee, R.G., van Donkelaar, P., 1995. Mechanisms underlying functional recovery following stroke. Can. J. Neurol. Sci. 22, 257–263. http://dx.doi.org/10.1017/S0317167100039445.
Lin, T.N., Sun, S.W., Cheng, W.M., Li, F., Chang, C., 2002. Dynamic changes in cerebral blood flow and angiogenesis after transient focal cerebral ischemia in rats: evaluation with serial magnetic resonance imaging. Stroke 33, 2985–2991. http://dx.doi.org/10.1161/01.STR.0000037675.97888.9D.
Lin, C.Y., Chang, C., Cheung, W.M., Lin, M.H., Chen, J.J., Hsu, C.Y., Chen, J.H., Lin, T.N., 2008. Dynamic changes in vascular permeability, cerebral blood volume, vascular density, and size after transient focal cerebral ischemia in rats: evaluation with contrast-enhanced magnetic resonance imaging. J. Cereb. Blood Flow Metab. 28, 1491–1501. http://dx.doi.org/10.1038/jcbfm.2008.42.
van Lookeren Campagne, M., Thomas, G.R., Thibodeaux, H., Palmer, J.T., Williams, S.P., Lowe, D.G., van Bruggen, N., 1999. Secondary reduction in the apparent diffusion coefficient of water, increase in cerebral blood volume, and delayed neuronal death after middle cerebral artery occlusion and early repercussion in the rat. J. Cereb. Blood Flow Metab. 19, 1354–1364. http://dx.doi.org/10.1097/00004647-199912000-00009.
Martin, A., Macé, E., Boisgard, R., Montaldo, G., Thézé, B., Tanter, M., Tavitian, B., 2012. Imaging of perfusion, angiogenesis, and tissue elasticity after stroke. J. Cereb. Blood Flow Metab. 32, 1496–1507. http://dx.doi.org/10.1038/jcbfm.2012.49.
Montoya, C.P., Campbell-Hope, L.J., Pemberton, K.D., Dunnett, S.B., 1991. The "staircase test": a measure of independent forelimb reaching and grasping abilities in rats. J. Neurosci. Methods 36, 2–3. http://dx.doi.org/10.1016/0165-0270(91)90048-5.
Mohr, J.P., Grotta, J.C., Wolf, P.A., Moskowitz, M.A., Mayberg, M.R., Von Kummer, R., 2011. Stroke: Pathophysiology, Diagnosis, and Management. Elsevier Health Sciences.
Murphy, T.H., Corbett, D., 2009. Plasticity during stroke recovery: from synapse to behaviour. Nat. Rev. Neurosci. 10, 86–187. http://dx.doi.org/10.1038/nrn2735.
Neelin, Fonov et al. Copyright © 1997–2016. McConnell Brain Imaging Centre, MINCTools. ⟨http://www.bic.mni.mcgill.ca/ServicesSoftware/MINC⟩.
Neumann-Haefelin, T., Kastrup, A., de Crespigny, A., Yenari, M.A., Ringer, T., Sun, G.H., Moseley, M.E., 2000. Serial MRI after transient focal cerebral ischemia in rats: dynamics of tissue injury, blood-brain barrier damage, and edema formation. Stroke 31, 1965–1972. http://dx.doi.org/10.1161/01.STR.31.8.1965.
Nguemeni, C., Gomez-Smith, M., Jeffers, M.S., Schuch, C.P., Corbett, D., 2015. Time course of neuronal death following endothelin-1 induced focal ischemia in rats. J. Neurosci. Methods 242, 72–76. http://dx.doi.org/10.1016/j.jneumeth.2015.01.005.
Nishibe, M., Urban, E.T., 3rd, Barbay, S., Nudo, R.J., 2015. Rehabilitative training promotes rapid motor recovery but delayed motor map reorganization in a rat cortical ischemic infarct model. Neurorehabil. Neural Repair. 29, 472–482. http://dx.doi.org/10.1177/1545968314543499.
Olsen, T.S., Lassen, N.A., 1984. A dynamic concept of middle cerebral artery occlusion and cerebral infarction in the acute state based on interpreting severe hyperemia as a sign of embolic migration. Stroke 15, 458–468. http://dx.doi.org/10.1161/01.STR.15.3.458.
Paxinos, G., Watson, C., 2005. The Rat Brain in Stereotaxic Coordinates. fifth ed.
Rossini, P.M., Tecchio, F., Pizzella, V., Lupoi, D., Cassetta, E., Pasqualetti, P., 2001. Interhemispheric difference of sensory hand area after mono- hemispheric stroke: MEG/MRI integrative study. NeuroImage 14, 474–485. http://dx.doi.org/10.1006/nimg.2000.0686.
Seil, F.J., 1997. Recovery and repair issues after stroke from the scientific perspective. Curr. Opin. Neurol., 49–51. http://dx.doi.org/10.1097/00019052-199702000-00010.
Shen, Q., Du, F., Huang, S., Duong, T.Q., 2011. Spatiotemporal characteristics of postischemic hyperperfusion with respect to changes in T1, T2, diffusion, angiography, and blood-brain barrier permeability. J. Cereb. Blood Flow Metab. 31, 2076–2085. http://dx.doi.org/10.1038/jcbfm.2011.64.
Shih, Y.Y., Huang, S., Chen, Y.Y., Lai, H.Y., Kao, Y.C., Du, F., Hui, E.S., Duong, T.Q., 2014. Imaging neurovascular function and functional recovery after stroke in the rat striatum using forepaw stimulation. J. Cereb. Blood Flow Metab. 9, 1483–1492. http://dx.doi.org/10.1038/jcbfm.2014.103.
Speliotes, E.K., Caday, C.G., Do, T., Weise, J., Kowall, N.W., Finklestein, S.P., 1995. Increased expression of basic fibroblast growth factor (bFGF) following focal cerebral infarction in the rat. Brain Res. Mol. Brain Res. 29, 31–42. http://dx.doi.org/10.1016/0169-328X(95)00351-R.
Steinberg, B.A., Augustine, J.R., 1997. Behavioural, anatomical, and physiological aspects of recovery of motor function following stroke. Brain Res. Brain Res. Rev. 25, 125–132. http://dx.doi.org/10.1016/S0165-0173(97)00013-1.
Sternberg, S.R., 1983. Biomedical image processing. Computer 16, 2–34. http://dx.doi.org/10.1109/MC.1983.1654163.
Szpak, G.M., Lechowicz, W., Lewandowska, E., Bertrand, E., Wierzba-Bobrowicz, T.,

Dymecki, J., 1999. Border zone neovascularization in cerebral ischemic infarct. Folia Neuropathol. 37, 264–268.
Tecchio, F., Zappasodi, F., Tombini, M., Oliviero, A., Pasqualetti, P., Vernieri, F., Ercolani, M., Pizzella, V., Rossini, P.M., 2006. Brain plasticity in recovery from stroke: an MEG assessment. NeuroImage 32, 1326–1334. http://dx.doi.org/10.1016/j.neuroimage.2006.05.004.
Virley, D., Beech, J.S., Smart, S.C., Williams, S.C., Hodges, H., Hunter, A.J., 2000. A temporal MRI assessment of neuropathology after transient middle cerebral artery occlusion in the rat: correlations with behaviour. J. Cereb. Blood Flow Metab. 20, 563–582. http://dx.doi.org/10.1097/00004647-200003000-00015.
Wang, L., Yushmanov, V.E., Liachenko, S.M., Tang, P., Hamilton, R.L., Xu, Y., 2002. Late reversal of cerebral and water diffusion after transient focal ischemia in rats. J. Cereb. Blood Flow Metab. 22, 253–261. http://dx.doi.org/10.1097/00004647-200203000-00002.
Wegener, S., Weber, R., Ramos-Cabrer, P., Uhlenkueken, U., Sprenger, C., Wiedermann, D., Villringer, A., Hoehn, M., 2006. Temporal profile of T2-weighted MRI distinguishes between pannecrosis and selective neuronal death after transient focal cerebral ischemia in the rat. J. Cereb. Blood Flow Metab. 26, 38–47. http://dx.doi.org/10.1038/sj.jcbfm.9600166.
White, F.C., Bloor, C.M., 1992. Coronary vascular remodelling and coronary resistance during chronic ischemia. Am. J. Cardiovasc. Pathol. 4, 193–202. http://dx.doi.org/10.1016/0022-2828(91)91345-R.
Wesson, D.W., Wilson, D.A., 2011. Sniffing out the contributions of the olfactory tubercle to the sense of smell: hedonics, sensory integration, and more? Neurosci. Biobehav. Rev. 35, 655–668. http://dx.doi.org/10.1016/j.neubiorev.2010.08.004.
Windle, V., Szymanska, A., Granter-Button, S., White, C., Buist, R., Peeling, J., Corbett, D., 2006. An analysis of four different methods of producing focal cerebral ischemia with endothelin-1 in the rat. Exp. Neurol. 201, 324–334. http://dx.doi.org/10.1016/j.expneurol.2006.04.012.
Womelsdorf, T., Valiante, T.A., Sahin, N.T., Miller, K.J., Tiesinga, P., 2014. Dynamic circuit motifs underlying rhythmic gain control, gating and integration. Nat. Neurosci. 17, 1031–1039. http://dx.doi.org/10.1038/nn.3764.
Yu, S.W., Friedman, B., Cheng, Q., Lyden, P.D., 2007. Stroke-evoked angiogenesis results in a transient population of microvessels. J. Cereb. Blood Flow Metab. 27, 755–763. http://dx.doi.org/10.1038/sj.jcbfm.9600378.
Zhang, P., Yu, H., Zhou, N., Zhang, J., Wu, Y., Zhang, Y., Bai, Y., Jia, J., Zhang, Q., Tian, S., Wu, J., Hu, Y., 2013. Early exercise improves cerebral blood flow through increased angiogenesis in experimental stroke rat model. J. Neuroeng. Rehabil. 10, 1–10. http://dx.doi.org/10.1186/1743-0003-10-43.
van der Zijden, J.P., van der Toorn, A., van der Marel, K., Dijkhuizen, R.M., 2008. Longitudinal in vivo MRI of alterations in peri-lesional tissue after transient ischemic stroke in rats. Exp. Neurol. 212, 207–212. http://dx.doi.org/10.1016/j.expneurol.2008.03.027.